

Dynamic Numerical Analysis of the Safety of Pedestrian Bridges in the Influence Zone of Metro Stations

Ke Ji, Boi-Yee Liao*

Department of Engineering, International College, Krirk University, Thailand

Received August 14, 2025; Revised November 20, 2025; Accepted December 22, 2025

Cite This Paper in the Following Citation Styles

(a): [1] Ke Ji, Boi-Yee Liao, "Dynamic Numerical Analysis of the Safety of Pedestrian Bridges in the Influence Zone of Metro Stations," *Civil Engineering and Architecture*, Vol. 14, No. 1, pp. 331 - 355, 2026. DOI: 10.13189/cea.2026.140121.

(b): Ke Ji, Boi-Yee Liao (2026). *Dynamic Numerical Analysis of the Safety of Pedestrian Bridges in the Influence Zone of Metro Stations*. *Civil Engineering and Architecture*, 14(1), 331 - 355. DOI: 10.13189/cea.2026.140121.

Copyright©2026 by authors, all rights reserved. Authors agree that this article remains permanently open access under the terms of the Creative Commons Attribution License 4.0 International License

Abstract With the rapid development of urban rail transit, the impact of subway station construction on the structural safety of adjacent pedestrian bridges has garnered significant attention. Existing studies often focus on single aspects like dynamic monitoring or finite element simulation, lacking a comprehensive framework. This study aims to address the gap by proposing an integrated technical framework combining "three-dimensional finite element dynamic simulation – support structure optimization – on-site real-time monitoring." Using the Memorial Hall Station of Metro Line 13 as a case study, a composite support system was designed for specific strata (argillaceous siltstone, fully weathered silty clay), capable of withstanding vertical and horizontal pressures of 113.84 kPa and 78.81 kPa, respectively. A refined 3D finite element model was established using Midas Gen 2022. Results demonstrate that the optimized support system effectively controls deformation: maximum foundation displacements in X, Y, and Z directions were 1.6 mm, 2.5 mm, and 39.6 mm, respectively, and the maximum bending moment change in the steel box girder was ≤ 14.9 kN·m/m, all within code limits. The "pre-support pipe shed + step-by-step excavation" method limited differential settlement to 2.1 mm, far below the specification limit of 127 mm. On-site monitoring data showed 92% consistency with simulation results. This integrated framework ensures pedestrian bridge safety during subway construction, providing a technical reference for similar urban underground projects near existing structures.

Keywords Rail Transit Impact, Simulation Technique, Pedestrian Bridge, Structural Mechanics

1. Introduction

With the rapid development of urban rail transit system, the impact of the construction of rail transit station platforms on the surrounding existing structures has been increasingly concerned, and the safety and stability of footbridges, as an important part of urban transportation, are directly related to the travel safety of pedestrians. As shown in Figure 1, it presents the finite element calculation model of the urban footbridge structure. For details on this model, please refer to related studies [1,2].

During the construction of rail transit platforms, the surrounding footbridges are often significantly affected by construction activities such as pit excavation and viaduct construction [3,4]. Xue Chenyu et al. [5] evaluated the dynamic response of large-scale pedestrian suspension bridges during subway platform construction in terms of settlement and deformation. This was done using a robotic total station (RTS) and geodetic GNSS receivers, and this work also tested a large footbridge during subway construction with a low-power GNSS receiver. This proves that low-cost GNSS sensors can monitor structural movements at frequencies of 1–3 Hz.

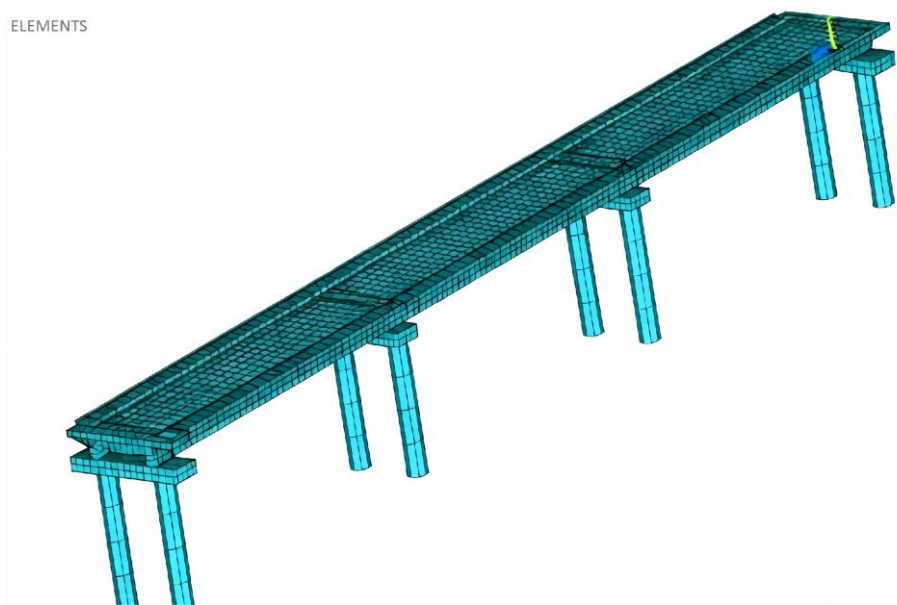


Figure 1. Finite element calculation model of urban footbridge structure. Source: Zheng H (2015)

A ElSafty et al. [6] used vibrating-wire sensors with integrated thermistors to monitor the dynamic strains in BFRP rods in the link plates of a pedestrian bridge deck during pavement construction. The results showed that the BFRP rods in the link plates are subjected to smaller strains compared to the strain at BFRP cracking. In recent years, three-dimensional force simulation analysis, as an advanced engineering analysis tool, has played an important role in predicting and assessing the impact of construction activities on existing structures. By using computer simulation technology, the impact of construction activities on the force state of the footbridge can be predicted more accurately, so as to provide a scientific basis for the optimization of the construction plan and the protection of the footbridge [7,8].

Hussein Muhammad et al. [9] used two types of finite element models, namely OMA and FEM, to evaluate the dynamic characteristics of the ultra-high-performance fiber-concrete footbridge structure under external vibration. The results show that there is a significant variation in the intrinsic frequency between the two methods and a strong correlation between the finite element models with very similar vibration patterns. Bryan Castillo et al. [10] tested how a footbridge responds to external structural interaction (HSI) using real-time hybrid simulation (RTHS). The results showed that there was a significant dynamic coupling between the loads and the structural response, with the fundamental frequency of transverse vibration being about 1.0 Hz and the peak of vertical vibration being close to 2.0 Hz. Juan D. Aux et al. [11] proposed a new predictive model for human-structure interaction (HSI), which integrates a three-dimensional biomechanical model of the human body and represents the pedestrian bridge as a simply-supported Euler-Bernoulli beam (using the beam's fundamental frequency as the base). This model employs

inverse dynamics and can accurately capture 3D gait and its interaction with structural vibration.

During subway station construction, excavation activities cause soil stress release, leading to soil settlement and lateral displacement. This soil deformation is transmitted to the adjacent pedestrian bridge pile foundation, resulting in the displacement and stress change in the bridge superstructure. In severe cases, it may cause structural damage to the pedestrian bridge.

To address the research gaps and highlight the contributions of this study, the novelty lies in three aspects: (1) Proposing a coupled analysis method of subway construction and pedestrian bridge structural safety that considers dynamic construction processes; (2) Developing an optimized support system suitable for complex strata (muddy siltstone and fully weathered powdery clay) to effectively control structural deformation; (3) Realizing the dynamic correction of the simulation model through real-time monitoring data, improving the accuracy of safety evaluation.

Based on existing research, this work addresses the unsafe construction factors generated by structural engineering projects on a footbridge during the construction of a rail transit station concourse by constructing an accurate three-dimensional model to simulate various force conditions during the construction process, analyzing key indicators such as settlement, deformation, and stress distribution of the footbridge during the construction process, and then evaluating the degree of impact of construction activities on the safety and stability of the footbridge. This study not only has important theoretical value, but also can provide useful reference for the design of construction programs and the formulation of protection measures for flyovers in actual projects.

2. Construction Conditions

The No. 3 shaft is located on the north side of the subway station, with a bottom depth of approximately 32.00m. It is constructed using the inverted shaft wall method, and the proposed support system includes anchor rods or grouting anchor pipes, grating steel frames, reinforcing steel meshes, and shotcrete. The cross-channel is constructed using an upper and lower bench method. Its support system consists of anchor rods, steel frames, wire mesh, and shotcrete, with additional large pipe sheds and small conduits pre-installed at the arch.

No. 1 pedestrian bridge crosses West Dongfeng Road. Its main span is approximately 40.5m in length, 4.4m in width, and the ladder section is 3.0m in width. The main span structure is a pre-supported spliced steel box girder bridge, the height of the box girder is 0.9m~1.4m, and the main span is supported by two foundations, and these foundations are built on drilled grouting piles. The footbridge crosses the Memorial Hall subway station of Line 13, and the pile foundation of the No.3 shaft, cross passage and hall of the subway station is adjacent to the No.1# footbridge. The minimum horizontal clearance between the No. 3 shaft and the pedestrian bridge's pile foundation is 19.1m; between the No. 3 cross passage and the pedestrian bridge's pile foundation is 15.7m; between the sidewalls of the subway station's guide hole and the north-side pedestrian bridge's pile foundation is 6.0m; between the sidewalls of the subway station's guide hole and the south-side pedestrian bridge's pile foundation is 6.0m; and the sidewalls of the guide hole of the subway station and the pile foundation of the footbridge on the south side is 6.0m. The minimum horizontal clearance between the side wall of the subway station guide hole and the south-side pedestrian bridge's pile foundation is 3.4m. Entrance/Exit G's flat section passes through the piles of the bridge's step section with a net distance of 0.86m. The step section's construction also overlaps with the bottom of 6 main-span piles. During excavation, these piles will be cut.

3. Engineering Geology

3.1. Topography of the Site

The line of this site mainly travels along Dongfeng Road, crossing municipal roads, underground tunnels, human defense projects, elevated bridges, etc., and the ground conditions are complicated. Dongfeng Road is an important east-west traffic artery, with busy traffic along the route, large flow of people and vehicles, and very complicated underground pipelines; the municipal paving construction on both sides of the road was completed at the end of last year. Since most boreholes were on the main road and sidewalks, the work was really tough; some of the

holes had to be moved to different spots during the actual work. The project site is an argillaceous depression formed from the Late Paleozoic to the Middle Triassic. In this area, approximately 7,000 meters thick of monolithic clastic formations, carbonate formations, and coal-bearing formations have been deposited, with the deposition center located in the Huadu area. The Indo-Chinese movement has led to transitional folding of the Late Paleozoic strata in this area and the development of strike fractures. The direction of the tectonic line is dominated by the northeast and east-west directions, and these two directions often combine to form an "S"-shaped bend. The Mesozoic and Cenozoic eras were characterized by the development of fault basins and the distribution of deep and large fracture zones. The Mesozoic era was characterized by frequent magmatic activities, with multiple intrusions and overflows, while the Cenozoic era was mainly characterized by overflows of basic alkaline magma.

3.2. Engineering Geological Analysis near Memorial Hall Station and #1 Pedestrian Bridge

The drilling arrangement of No.3 shaft, cross passage and subway station hall section of Memorial Hall Station is shown in Figure 2, and the geological stratification is illustrated in Figure 3.

(1) The engineering importance level of this line is Grade I, the site complexity level is Grade II, the environmental risk level of the project surroundings is Grade I, and the grade of geotechnical engineering investigation is Grade A. (2) The survey of rocks and underground structures at this site and the nearby area shows that the ground here is generally stable. There are no geological hazards such as landslides, mudslides, or avalanches, and the potential undesirable geologies mainly consist of ground subsidence and liquefaction of sandy soils, which can be constructed on the construction site after treatment. (3) From top to bottom, the main strata along the line are fill, fine sand, silt, silty soil, silty clay, and residual silty clay deposits. The underlying bedrock is mainly Cretaceous clastic rock, primarily argillaceous siltstone. (4) The fill layer <1>, plastic silty clay layer <4N-2>, silt layer <4-2A>, silty clay layer <4-2B>, and residual silty clay layer <5N> are weakly permeable and weakly water-bearing; the fine silty sand layer <3-1> is moderately permeable and strongly water-bearing; and the strongly weathered, moderately weathered, and slightly weathered bedrock layers are weakly permeable due to uneven fissure development. (5) Weak strata such as the artificial fill layer <1>, fine sand layer <3-1>, silt layer <4-2A>, and silty soil layer <4-2B> exist in the shallow part of the site and are prone to collapse. Therefore, the design should include effective measures to protect the shaft walls. (6) According to the corrosivity analysis results of 6 groups of groundwater samples and 6 groups of surface soil samples, the groundwater at this site is slightly corrosive to concrete structures and to the steel

Table 8. Initial support load of the bottom support of the underground excavation Type III section tunnel

Geological borehole number	MM2Z3-JNT-11						
Stratum	1-2	4-2B	5N-1	6.00	7-3	8-3	Total
Thickness (m)	5.224	1.80	6.60	11.6	1.876	0.00	27.1
Unit weight (kN/m ³)	19.1	15.3	19.9	20.6	19.6	25.3	
Floating unit weight (kN/m ³)	9.10	5.30	9.90	10.6	9.60	15.3	
Internal friction angle (°)	10	16.5	20.2	24.2	28.0	32.0	
Lateral pressure coefficient	0.50	0.45	0.45	0.33	0.33	0.25	0.42
Surface overload (kPa)	20						
vertical earth pressure (kPa)	47.54	9.54	65.34	122.96	18.01	0.00	110.65
Lateral earth pressure (kPa)							103.99
Lateral overload (kPa)							6.60

Table 9. Initial support load at the vault of the underground excavation Type IV section tunnel

Geological borehole number	MM2Z3-JNT-48					
Stratum	1-2	4N-2	5N-1	0.00	0.00	Total
Thickness (m)	4.650	0.700	0.000	0.000	0.000	
Unit weight (kN/m ³)	19.1	15.3	19.9	0.00	0.00	
Floating unit weight (kN/m ³)	9.10	5.30	9.90	0.00	0.00	
Internal friction angle (°)	10.00	16.50	20.20	0.00	0.00	
Lateral pressure coefficient	0.50	0.45	0.45	0.00	0.00	0.91
Surface overload (kPa)	20					
vertical earth pressure (kPa)	42.32	3.71	0.00	0.00		46.03
Lateral earth pressure (kPa)						22.83
Lateral overload (kPa)						9.00

Table 10. Initial support load of the bottom support of the underground excavation Type IV section tunnel

Geological borehole number	MM2Z3-JNT-48						
Stratum	1-2	4N-2	5N-1	0.0	0.0	0.0	Total
Thickness(m)	4.65	2.70	4.800	0.0	0.0	0.0	12.15
Unit weight (kN/m ³)	19.1	15.3	19.9	0.0	0.0	0.0	
Floating unit weight (kN/m ³)	9.1	5.30	9.90	0.0	0.0	0.0	
Internal friction angle (°)	10	16.5	20.20	0.0	0.0	0.0	
Lateral pressure coefficient	0.5	0.45	0.45	0.0	0.0	0.0	0.74
Surface overload (kPa)	20						
vertical earth pressure (kPa)	42.32	14.31	47.52	0.0	0.0	0.0	104.15
Lateral earth pressure (kPa)							48.98
Lateral overload (kPa)							9.00

4.3.3. Calculation Results

Figure 6 shows the basic combined bending moment diagram of each underground excavation tunnel section (Types I-IV) (Unit: kN m); Figure 7 illustrates the basic

shear force diagram of each underground excavation tunnel section (Types I-IV) (Unit: kN); Figure 8 shows the basic axial force diagram of each underground excavation tunnel section (Types I-IV) (Unit: kN).

Figure 9 shows the 3D finite element overall model; Station Hall Excavation Construction Work Setting; Figure 10 illustrates the 3# Shaft, Cross Passage and 11 shows the research flowchart.

Figure 9. 3D Finite Element Overall Model

Figure 10. 3# Shaft, Cross Passage and Station Hall Excavation Construction Work Setting

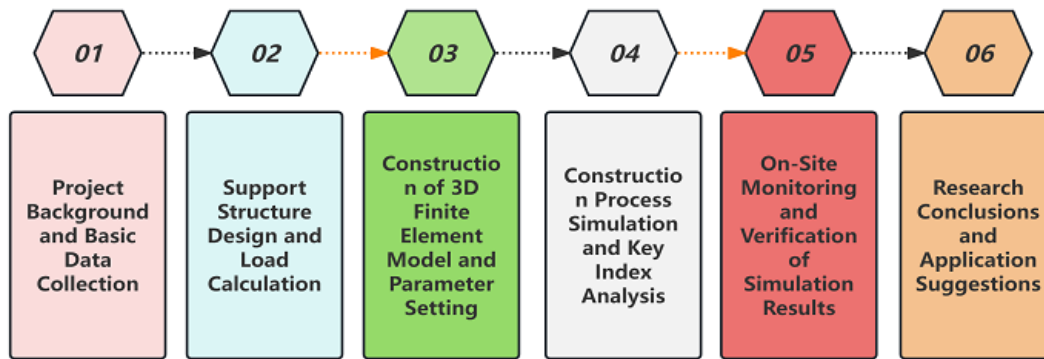


Figure 11. Research flowchart

Table 11. Material parameters

Materials	stockpile soil	silty soil	silty clay	fully weathered rock	moderately weathered rock	slightly weathered rock
Isomorphism (friction)	Coulomb	Coulomb	Coulomb	Coulomb	Coulomb	Coulomb
Capacity γ (KN/m ³)	19	17	18	21	26	26
Cohesion C (kPa)	17	8.4	19	34	500	700
Friction angle ϕ (°)	16	9.7	19	26	33	43
Elastic modulus E (MPa)	10	9	15	45	500	800
Poisson's ratio (μ)	0.3	0.3	0.35	0.23	0.18	0.18

Table 12. Construction Conditions

Construction Conditions	Main construction content
Condition 1	Analysis of the initial ground stress field at the site
Condition 2	Shaft No. 3 Reinforcement and Enclosure Construction
Condition 3	Excavation of the first layer of the shaft
Condition 4	Excavation of the first layer after the construction of overrunning small conduit support for the cross passageway
Condition 5	Construction of small guide hole overrun support
Condition 6	Second layer of shaft and cross passage excavation
Condition 7	Excavation of small guide hole
Condition 8	Construction of side piles and center columns of the subway station hall
Condition 9	Excavation of subway station hall
Condition 10	Excavation of the third level of shafts and cross passages
Condition 11	Excavation of MTR station hall to center slab
Condition 12	Shafts and cross passages excavation of the fourth and fifth levels
Condition 13	Excavation of MTR station concourse to base slab
Condition 14	Construction of subway station concourse floor, columns and side walls

The mechanical properties of the strata around the construction site play a key role in the force and deformation of the No. 1 pedestrian bridge during the construction of Memorial Hall Station's No. 3 shaft, cross passage, and subway station hall. Therefore, the calculation parameters should be reasonably selected based on the project's stratum distribution characteristics when conducting three-dimensional simulation. Material

parameters are shown in Table 11 and construction conditions in Table 12.

The stratum in the 3D finite element calculation model is mainly simplified based on the engineering geological data near the No.3 shaft of Memorial Hall Station, the cross passage, and the subway station hall. Additionally, the soil and rock parameters from drill hole MM2Z3-JNT-09 were selected for the 3D finite element model in this report. This

choice was made based on the borehole layout and its location relative to the project. Based on the data of this borehole, the rock strata mainly include vegetable fill, silty clay, powdery clay, fully weathered clay, and multiple layers of silty clay. According to the data of this borehole, the rock strata are mainly vegetation fill, silt loam, silty clay, fully weathered muddy siltstone, strongly weathered muddy siltstone, moderately weathered muddy siltstone, slightly weathered muddy siltstone, and so on, and the values of the calculation parameters of each stratum are mainly based on the relevant engineering geological investigation data and engineering experience [12,13], which are determined by comprehensive analysis as follows: the bottom of the model is constrained by the Z-direction displacement, the front and the back of the model are constrained by the Y-direction and the right and left surfaces of the model are constrained by the X-direction.

5.2. Simulation Results of the Impact of the Construction of the Subway Station Concourse at Memorial Hall Station on the Foundation of Pedestrian Bridge #1 and Its Analysis

Figure 12 illustrates the location of the proposed project and the steel box girders of the upper main span of No.1 footbridge. Figure 13-Figure 15 show the horizontal X-direction displacement, Y-direction displacement and Z-direction displacement of the box girder structure of the pile main span of No.1 footbridge under the key working conditions of the proposed project, while Figure 15 and Figure 16 show the X-direction and Y-direction bending moments of the box girder structure of the pile main span of No.1 footbridge during the construction of the proposed project. Figure 17 shows the cloud diagram of X-direction bending moment M_{yy} (kN m/m) of the box girder structure of the main span of No.1 footbridge pile during the construction of the proposed project.

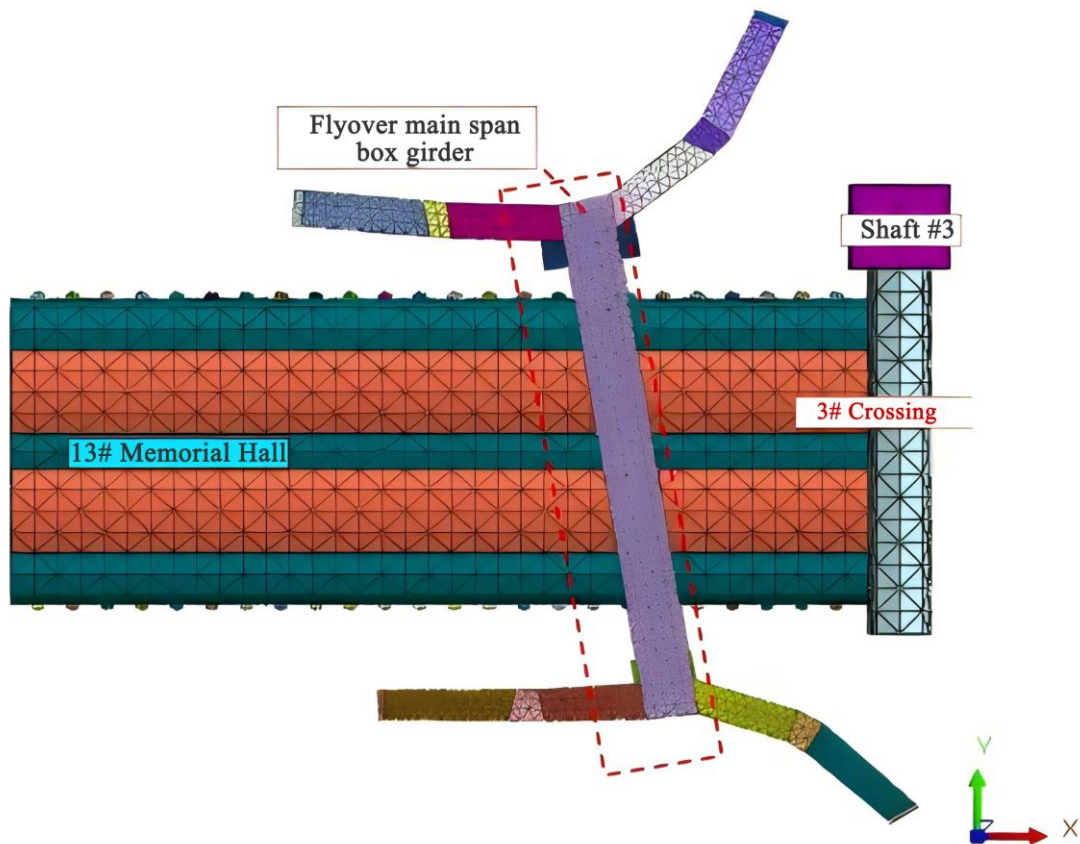
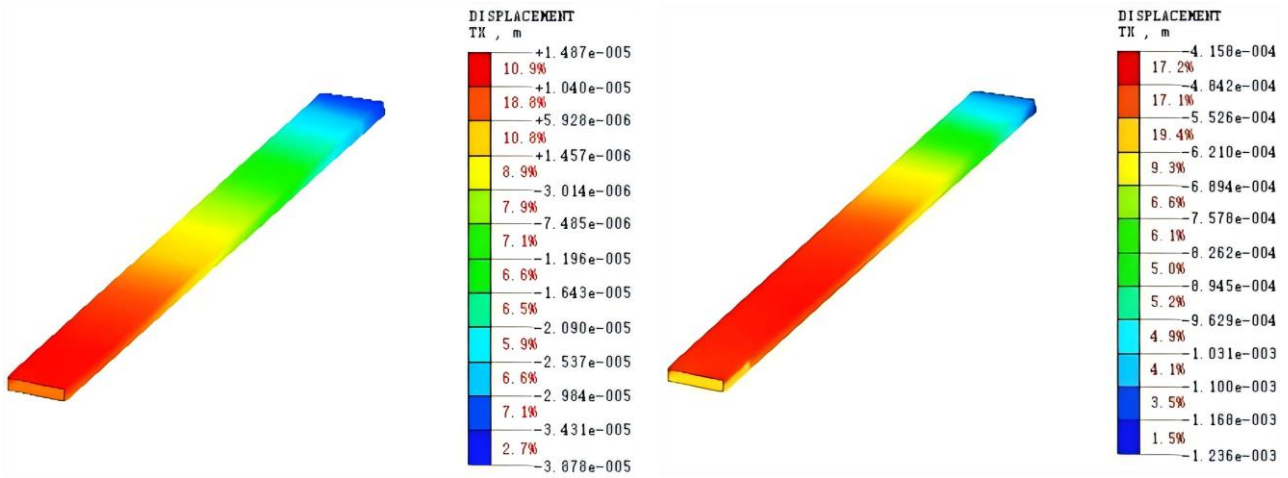
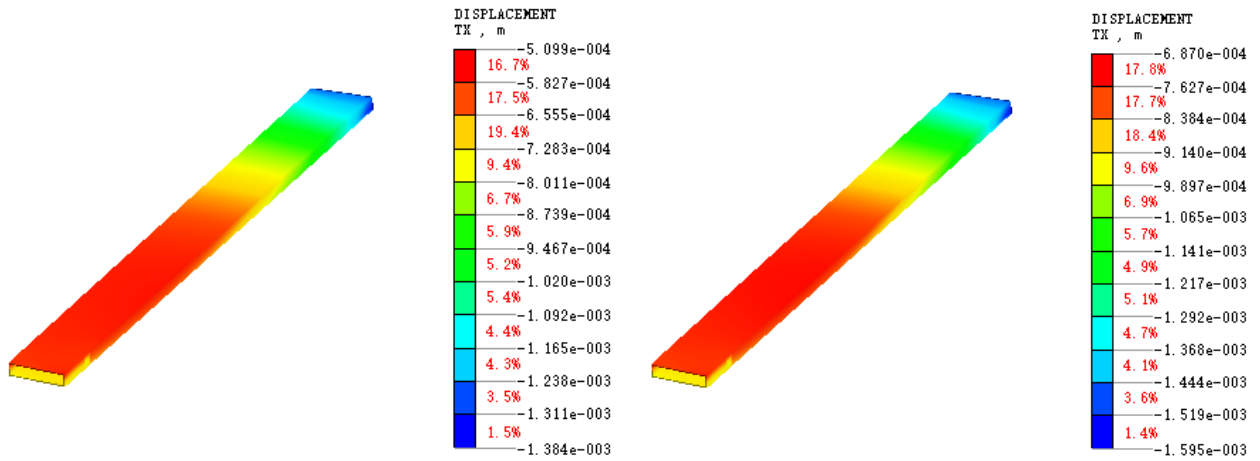


Figure 12. Description of the location of the proposed project and the upper main span steel box girder of the 1# pedestrian bridge



(1) Small auxiliary tunnels are excavated

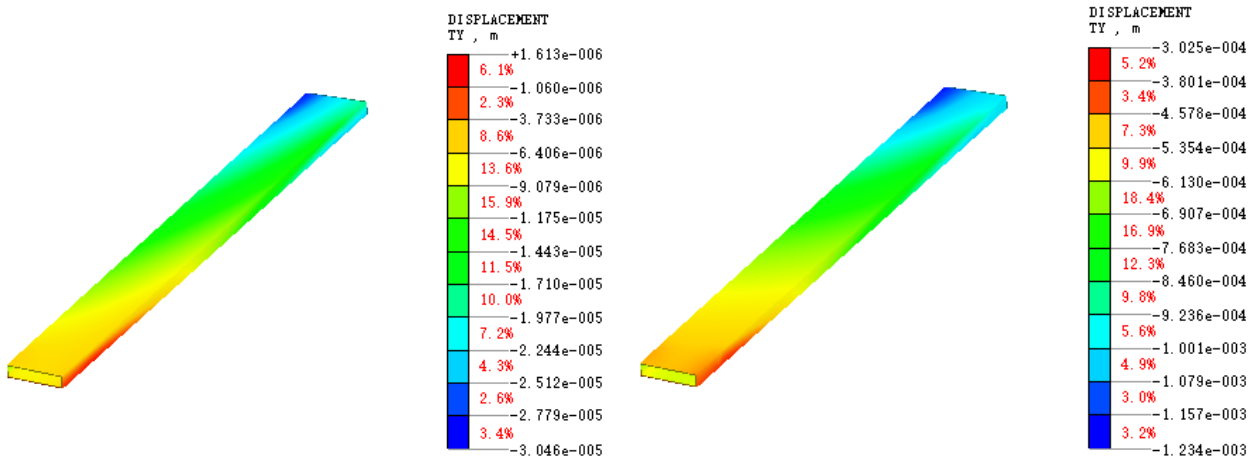
(2) Excavating the metro station lobby



(3) Excavate the subway station hall to the center plate position

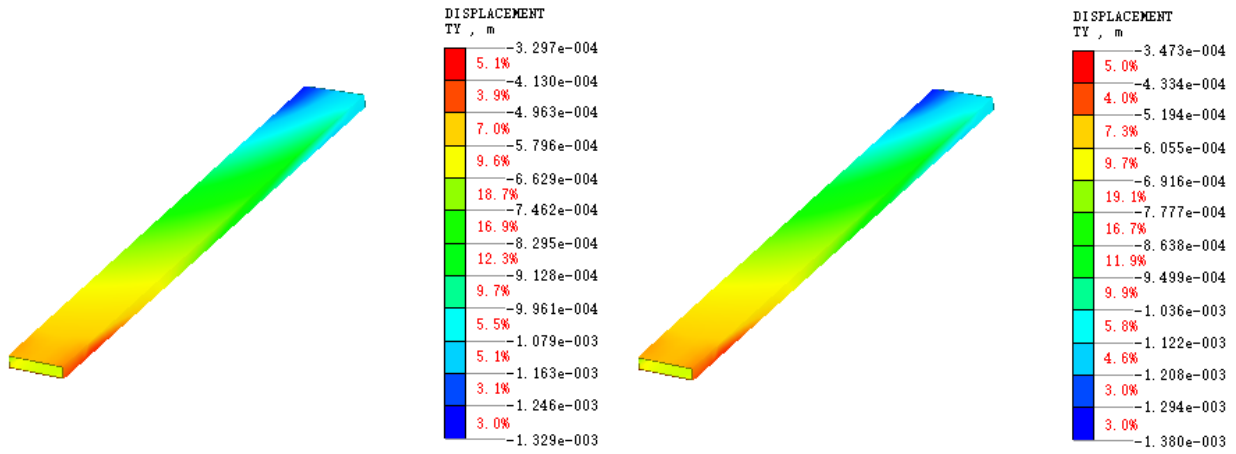
(4) Excavation of subway station hall to floor position

Figure 13. Horizontal X-direction displacement



(1) Small auxiliary tunnels are excavated

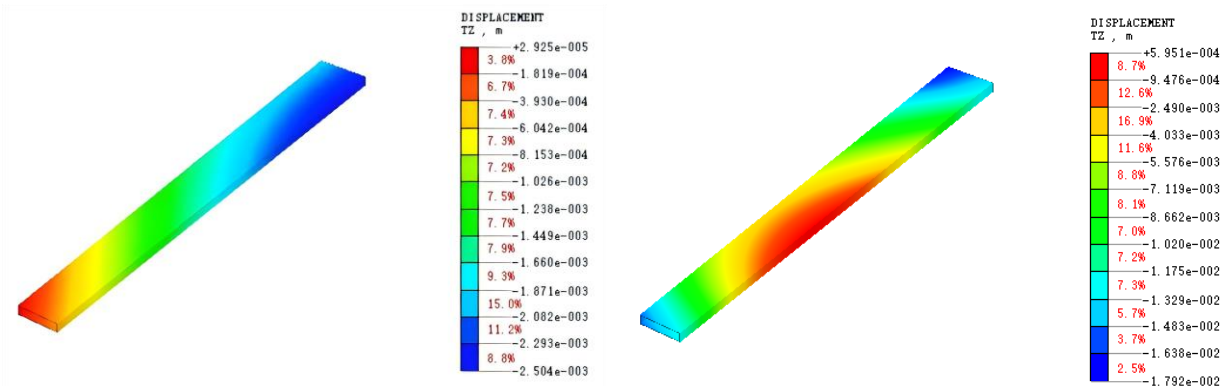
(2) Excavating the metro station lobby



(3) Excavate the subway station hall to the center plate position

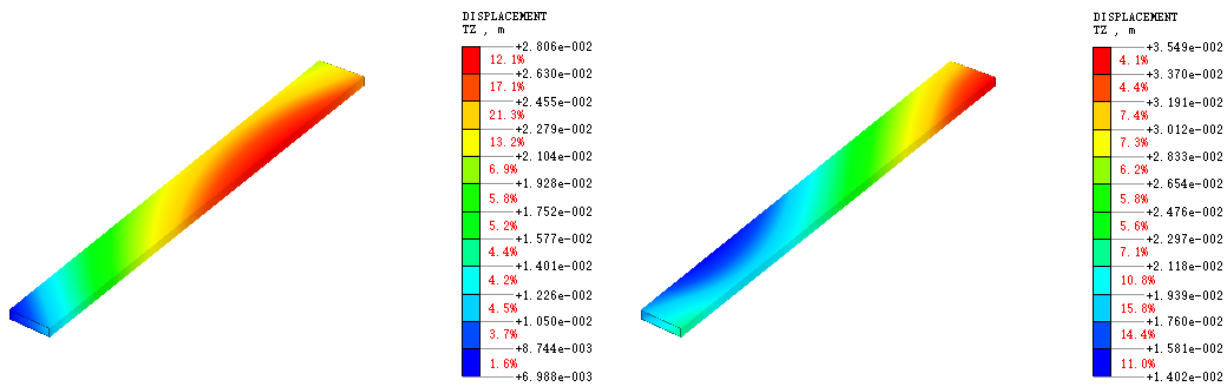
(4) Excavation of subway station hall to floor position

Figure 14. Horizontal Y-direction displacement



(1) Small auxiliary tunnels are excavated

(2) Excavating the metro station lobby



(3) Excavate the subway station hall to the center plate position

(4) Excavation of subway station hall to floor position

Figure 15. Horizontal Z-direction displacement

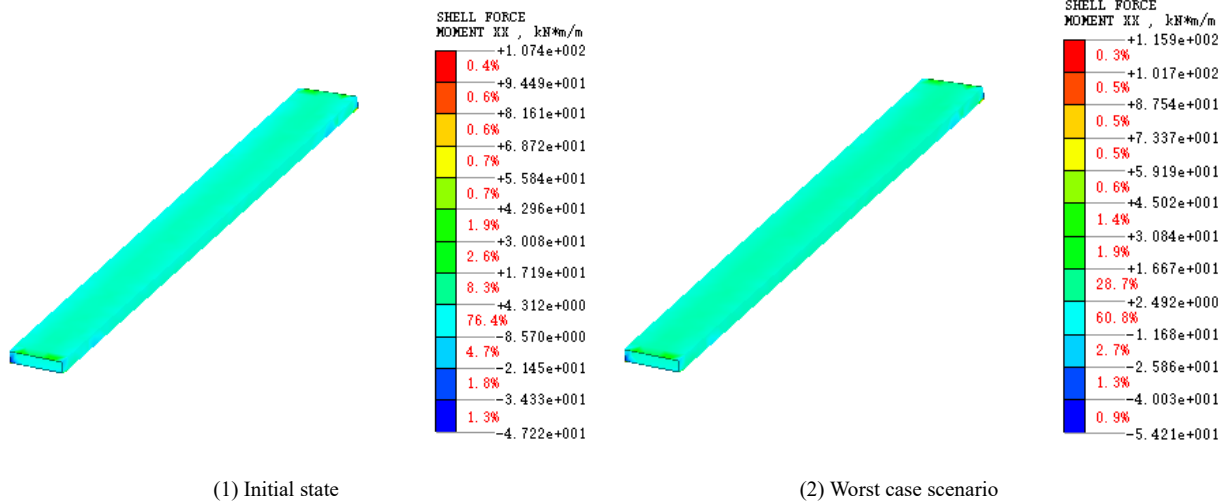


Figure 16. Cloud diagram of X-direction bending moment M_{xx} of the box girder structure of the main span of 1# footbridge pile during the construction of the proposed project (kN m/m)

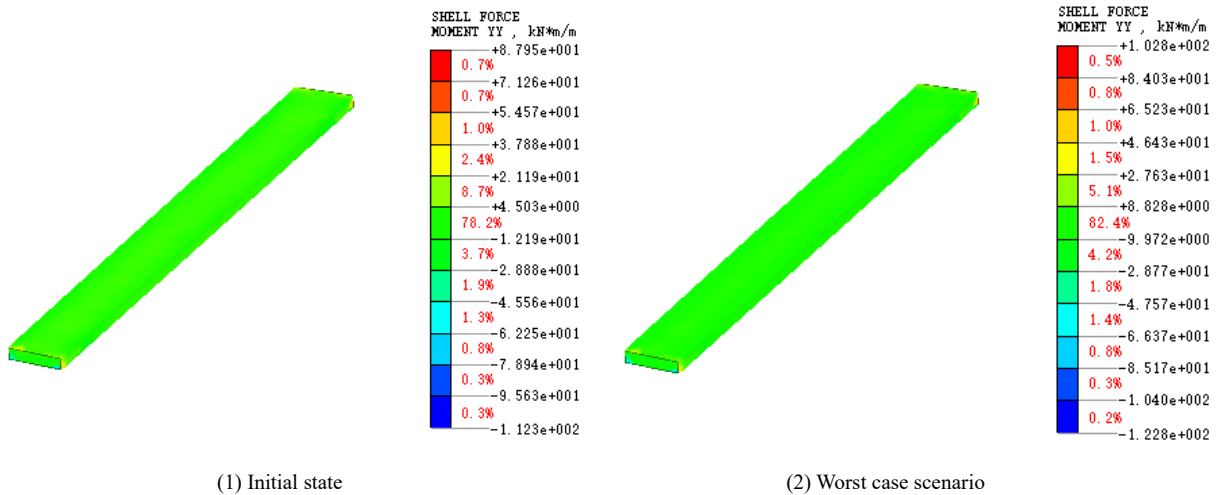


Figure 17. Cloud diagram of X-direction bending moment M_{yy} (kN m/m) of the box girder structure of the main span of No.1 footbridge pile during the construction of the proposed project

Table 13 summarizes the displacement of the superstructure of footbridge No. 1 under the critical working conditions during the construction of the proposed project. The three-dimensional simulation analysis results of the impact of Memorial Hall Station's No. 3 shaft, cross passage, and subway station hall construction process on the No. 1 pedestrian bridge's upper main span steel box girder structure show that: The construction process caused maximum displacements of 1.6 mm in the X-direction, 1.4 mm in the Y-direction, and 35.5 mm in the vertical direction in the steel box girder structure, with the total maximum displacement also being 35.5 mm. According to the force analysis of the main span box girder structure of the bridge, it is known that in the original state, the maximum positive bending moment (M_{xx}) in the X direction of the box girder structure of the bridge body and the shield tunnel structure is +107.4 kN m/m, the maximum negative bending moment is -47.2 kN m/m, the

maximum positive bending moment (M_{yy}) in the Y direction is +87.9 kN m/m, and the maximum negative bending moment is -47.1 kN m/m. Under the most unfavorable working condition, the maximum positive bending moment (M_{xx}) in the X direction of the bridge box girder structure and the maximum negative bending moment were +115.9 kN m/m and -54.2 kN m/m, while the maximum positive bending moment (M_{yy}) in the Y direction and the maximum negative bending moment were -122.8 kN m/m. The maximum positive bending moment in the Y direction was +102.8 kN m/m, and the maximum negative bending moment was -122.8 kN m/m. The maximum change of the maximum bending moment in the x direction and the Y direction was 14.9 kN m/m.

5.3. Simulation Results of the Impact of the Construction of the Subway Station Concourse at Memorial Hall Station on the Foundation of Pedestrian Bridge #1 and Its Analysis

Figure 18 shows the location of pile foundations on the north and south sides of the proposed project and footbridge No.1. Figure 19-Figure 21 show the displacement cloud diagrams of the pile foundations of footbridge No. 1 in the horizontal X direction, horizontal Y direction and vertical Z direction during the construction of shaft No. 3, the cross-channel and the concourse of the subway station. Table 14 summarizes the displacement of pile foundation of footbridge No. 1 under critical working conditions during the construction of the proposed project.

The 3D simulation analysis of the Memorial Hall Station No. 3 shaft, cross passage and subway station hall construction shows the following effects on the pile foundation of footbridge No. 1: the maximum vertical displacement reaches 39.6 mm, while horizontal displacements remain smaller at 1.0 mm in the X direction and 2.5 mm in the Y direction. The total maximum displacement is 39.7 mm. The maximum vertical displacement is 39.6 mm, and the maximum total displacement is 39.7 mm. According to the results of the 3D model, the maximum settlement of the pile foundations on the north and south sides of the adjacent foundations of footbridge No. 1 during the construction of the proposed project is 37.5 mm and 39.6 mm respectively, and the maximum settlement difference is 2.1 mm.

Table 13. Summary of the displacement of the superstructure of footbridge 1# under critical working conditions during the construction of the proposed project (mm)

Calculated working conditions	Maximum foundation displacement(mm)			
	X displacement	Y displacement	Z displacement	Total displacement
Analysis of initial ground stress field of the site	0.0	0.0	2.5	0.0
Excavation of small pilot hole	0.1	0.1	17.9	2.5
Excavation of subway station hall	1.2	1.2	28.1	17.9
Excavation of subway station hall to center slab	1.3	1.3 </td <td>35.5</td> <td>28.1</td>	35.5	28.1
Excavation of the subway station hall to the bottom slab	1.6	1.4	2.5	35.5

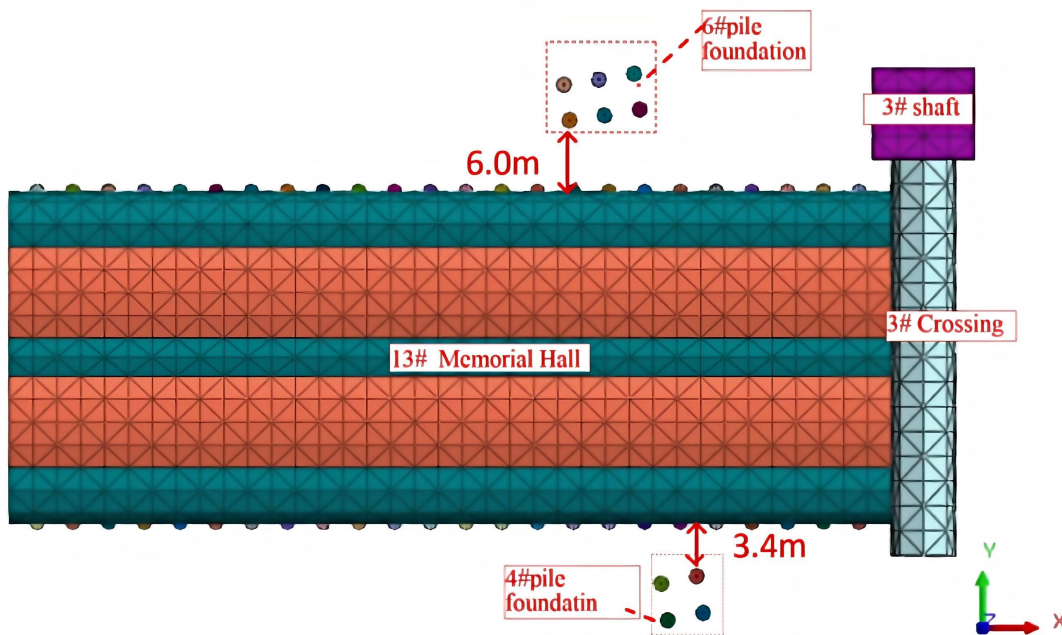
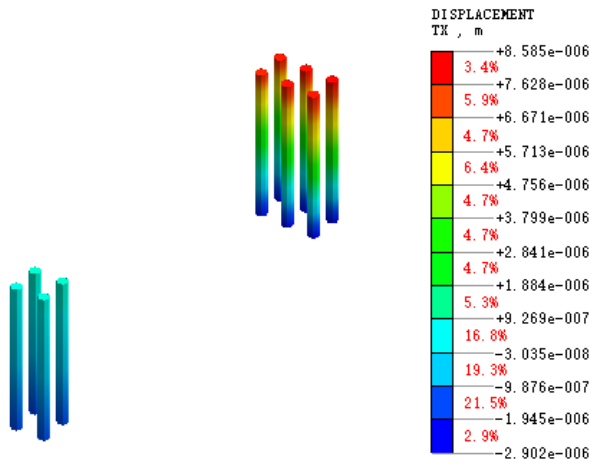
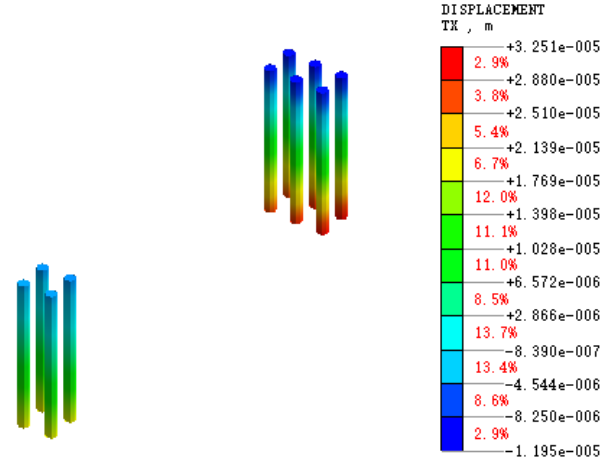


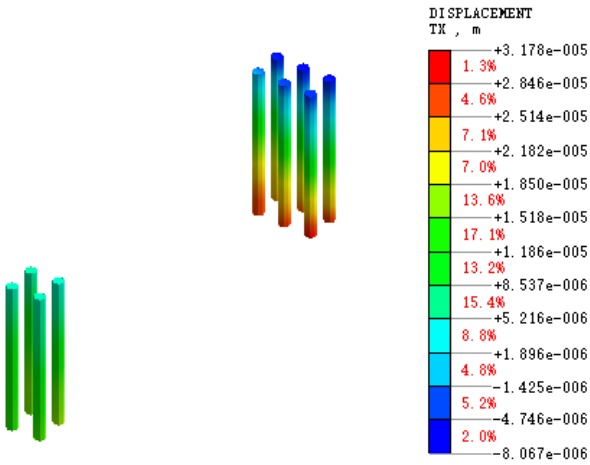
Figure 18. Description of Pile Locations North and South of Proposed Project and #1 Pedestrian Bridge



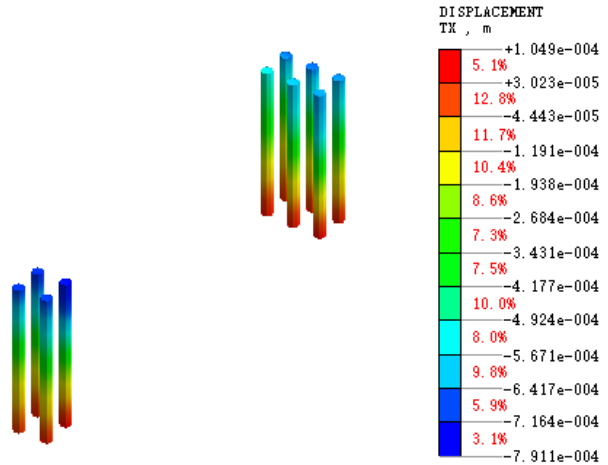
(1) Shaft 3 reinforcement and envelope construction



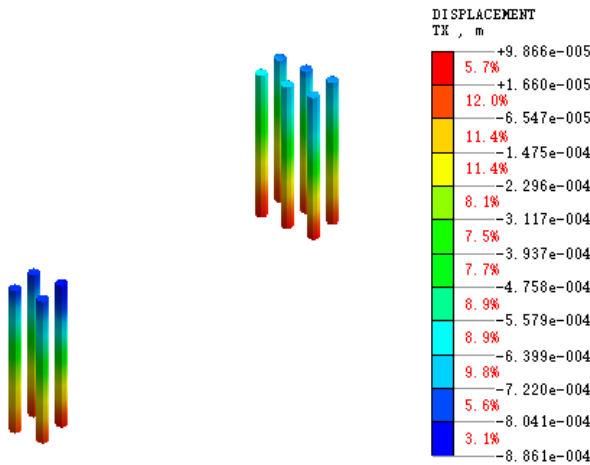
(4) Overrun Support Construction of Small Guide Hole



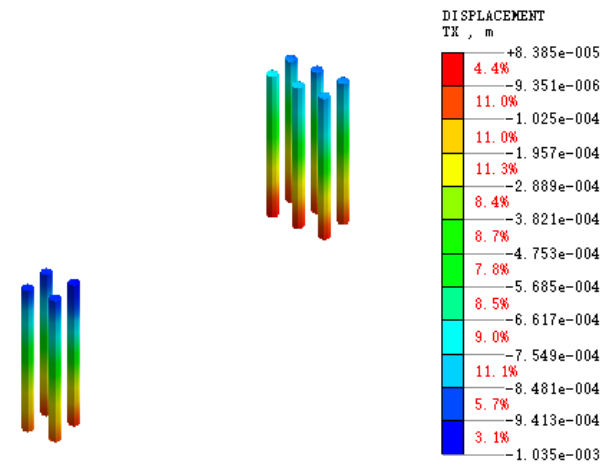
(6) Minor guide hole excavation



(8) Excavation of subway station halls

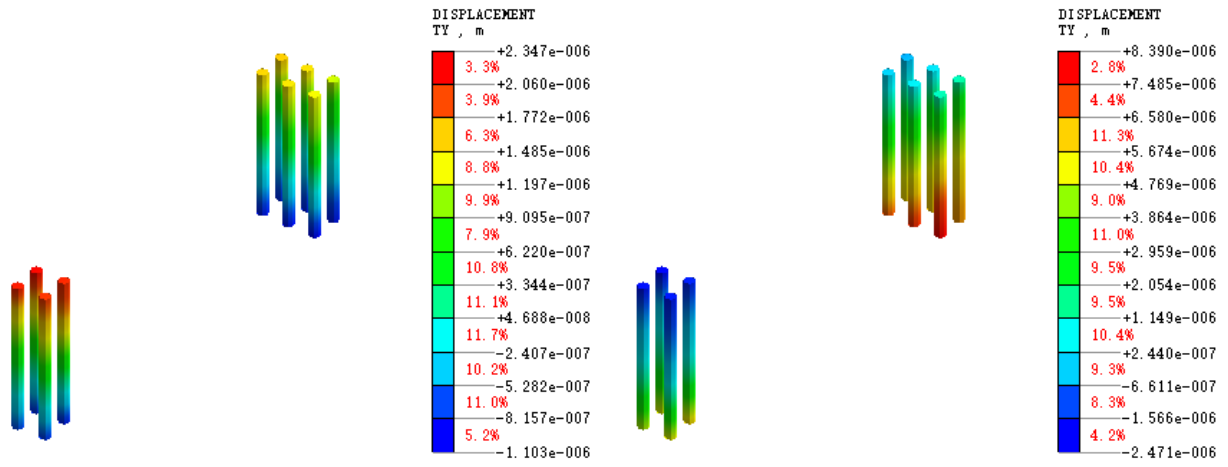


(10) Excavation of subway station concourse to centerboard location



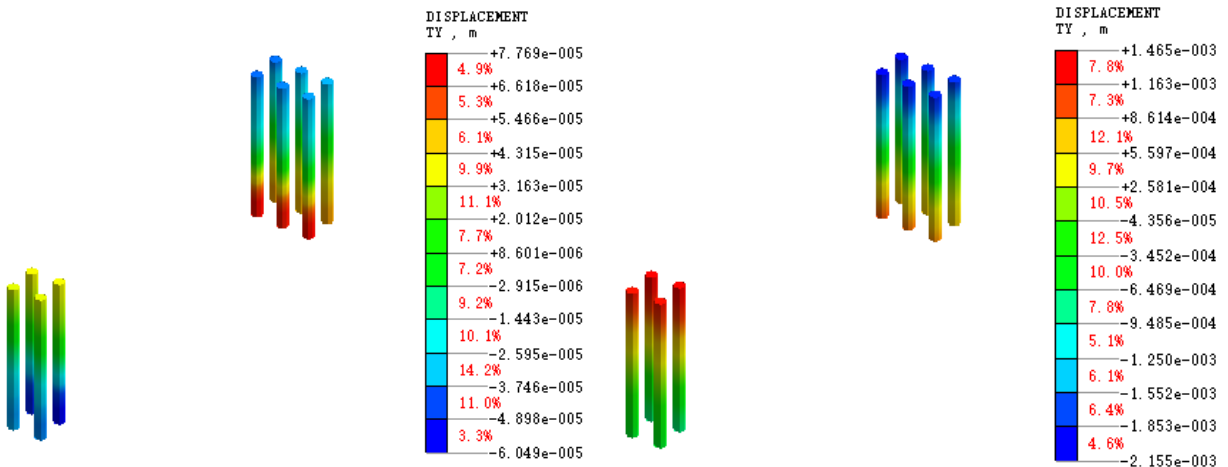
(12) Excavation of subway station concourse to footing position

Figure 19. Horizontal X-direction displacement



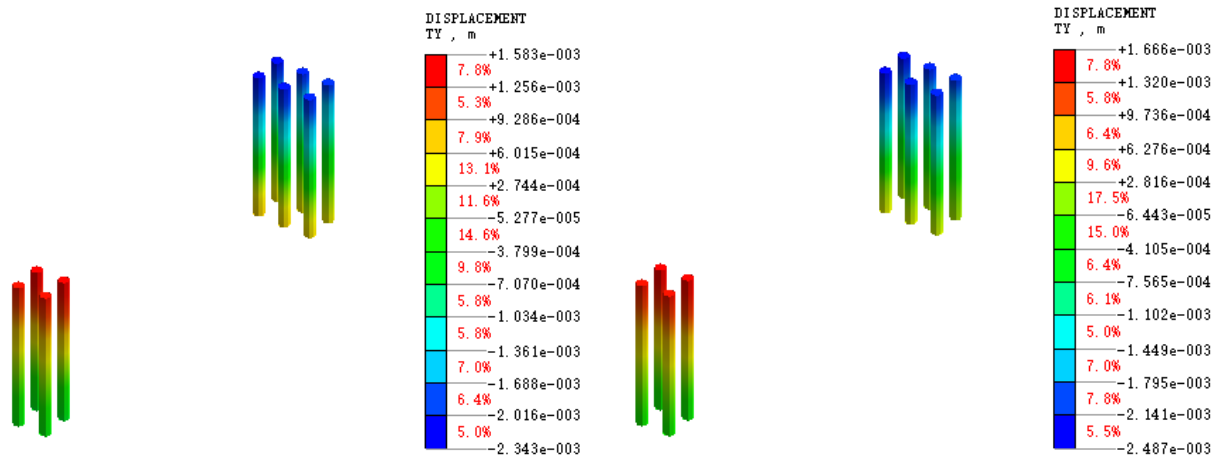
(1) Shaft 3 reinforcement and envelope construction

(4) Overrun Support Construction of Small Guide Hole



(6) Minor guide hole excavation

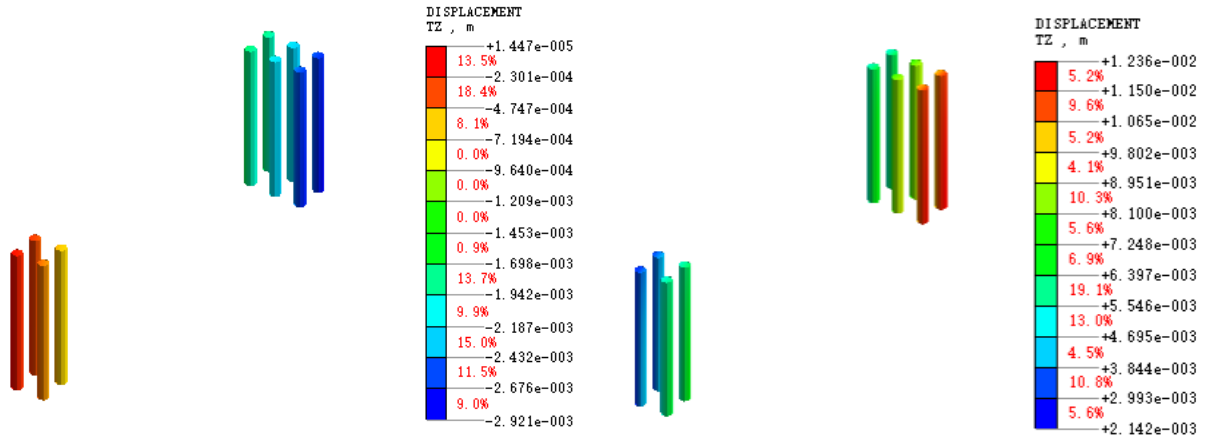
(8) Excavation of subway station halls



(10) Excavation of subway station concourse to centerboard location

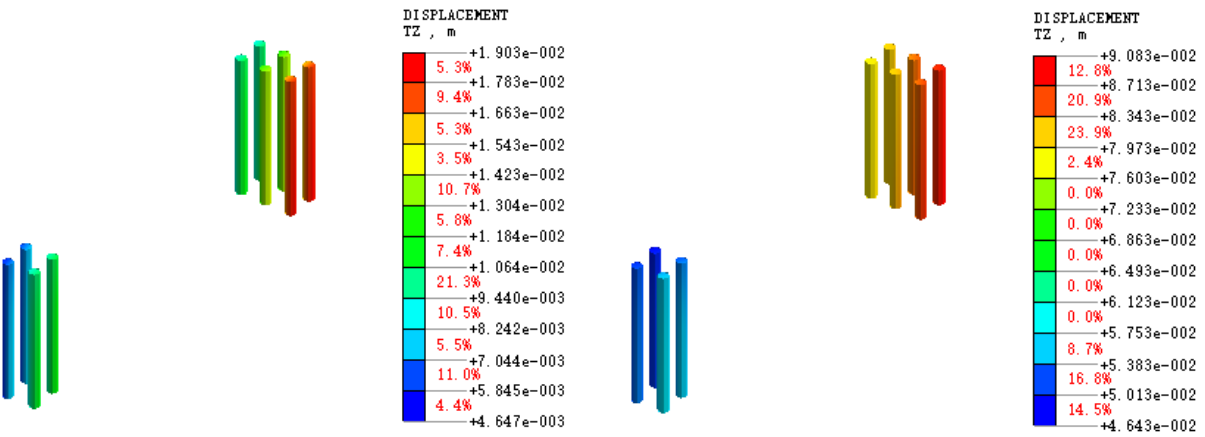
(12) Excavation of subway station concourse to footing position

Figure 20. Horizontal Y-direction displacement



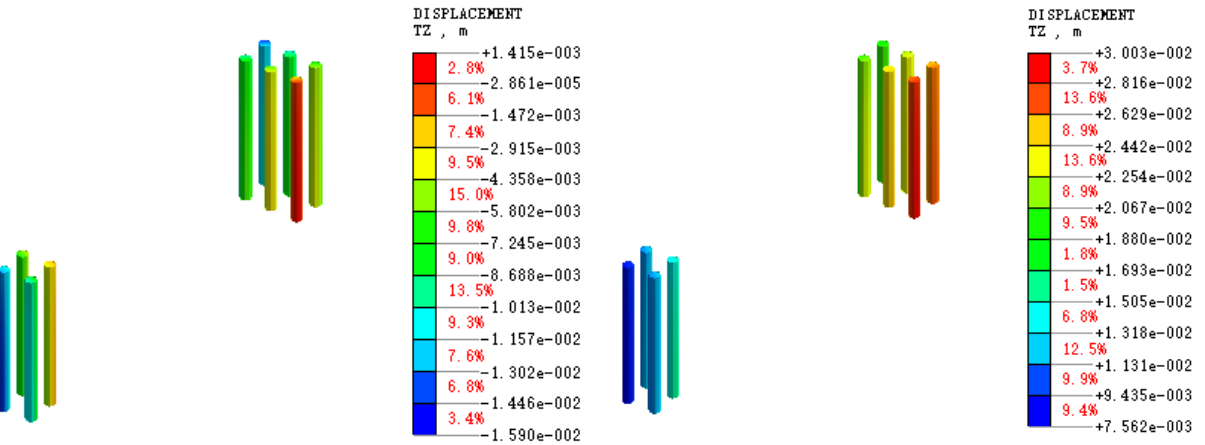
(1) Shaft 3 reinforcement and envelope construction

(4) Overrun Support Construction of Small Guide Hole



(6) Minor guide hole excavation

(8) Excavation of subway station halls



(10) Excavation of subway station concourse to centerboard location

(12) Excavation of subway station concourse to footing position

Figure 21. Horizontal Z-direction displacement

Table 14. Pile Displacement of 1# Pedestrian Footbridge under Critical Working Conditions during Construction of the Proposed Project (mm)

Calculated working conditions	Maximum foundation displacement(mm)			
	X displacement	Y displacement	Z displacement	Total displacement
Analysis of the initial ground stress field at the site	0.0	0.0	2.5	0.0
Shaft No. 3 Reinforcement and Enclosure Construction	0.1	0.1	2.9	2.9
Excavation of the first layer of the shaft	0.1	0.1	8.1	8.1
Excavation of the first layer after the construction of overrunning small conduit support for the cross passageway	0.1	0.1	13.6	13.6
Construction of small guide hole overrun support	0.1	0.1	12.4	12.4
Second layer of shaft and cross passage excavation	0.1	0.1	14.7	14.7
Excavation of small guide hole	0.1	0.1	19.0	19.0
Construction of side piles and center columns of the subway station hall	0.1	0.1	24.2	24.2
Excavation of subway station hall	0.8	2.1	25.3	25.3
Excavation of the third level of shafts and cross passages	0.8	2.2	26.4	26.4
Excavation of MTR station hall to center slab	0.9	2.3	30.1	30.1
Shafts and cross passages excavation of the fourth and fifth levels	0.9	2.3	37.1	37.1
Excavation of MTR station concourse to base slab	1.0	2.5	39.6	39.7
Construction of subway station concourse floor, columns and side walls	1.0	2.5	39.6	39.7

To summarize, the construction of shaft No. 3 of Memorial Hall Station, the cross passage and the subway station hall induced a certain amount of displacement of the pile foundation of footbridge No. 1. According to the Specification for the Maintenance of Highway Bridges and Culverts (JTG H11-2004) [14], the limit value of total settlement of pile foundation is $2.0\sqrt{l}=12.7\text{cm}$, and the limit value of horizontal displacement of pile foundation is $0.5\sqrt{l}=3.1\text{cm}$. In view of the fact that the displacement of pile foundation of No.1 footbridge induced by the construction of the proposed project is controllable, which is far less than the permissible value of foundation deformation stipulated in the specification, it is considered that the No.3 shaft, cross passage and subway station concourse of the Memorial Hall Station have a certain amount of displacement. Given that the displacement induced by the proposed construction is controllable and far less than the allowable foundation deformation stipulated in the specification, it is considered that the construction of No.3 shaft, cross passage and subway station hall of Memorial Hall Station will not jeopardize the safety of the pile foundation of No.1 footbridge. Therefore, it is considered that the construction of No.3 shaft, cross passage and subway station hall of Memorial Hall Station of Line 13 has less impact on the safety of the pile foundation of No.1 footbridge, and it is recommended to pay close attention to the monitoring data of the bridge foundation and carry out the informatization construction

in the course of construction.

5.4. Validation of the Finite Element Model

As illustrated in Figure 22 (Validation of the Finite Element Model with Field Monitoring Data), the accuracy and reliability of the simulation are confirmed through a comparative analysis of on-site monitoring data and the finite element model results.

Table 15 presents a comparison between the measured data of key monitoring points of the pedestrian overpass and the finite element simulation results. The monitoring data show that the cumulative variation of the overpass foundation during the construction period is controlled within a small range, which is in good agreement with the simulation results. This verifies the accuracy and reliability of the 3D finite element model in simulating the impact of construction.

(1) Static Validation: The calculated values of the steel box girder's bending moment and shear force are compared with the theoretical values obtained using the structural mechanics method, and the relative error is less than 5%, which confirms the accuracy of the static calculation.

(2) Dynamic Validation: The field monitoring data of the pedestrian bridge's natural frequency (measured by the ambient vibration test) is compared with the simulation results, and the relative error is less than 3%, which verifies the reliability of the dynamic model.

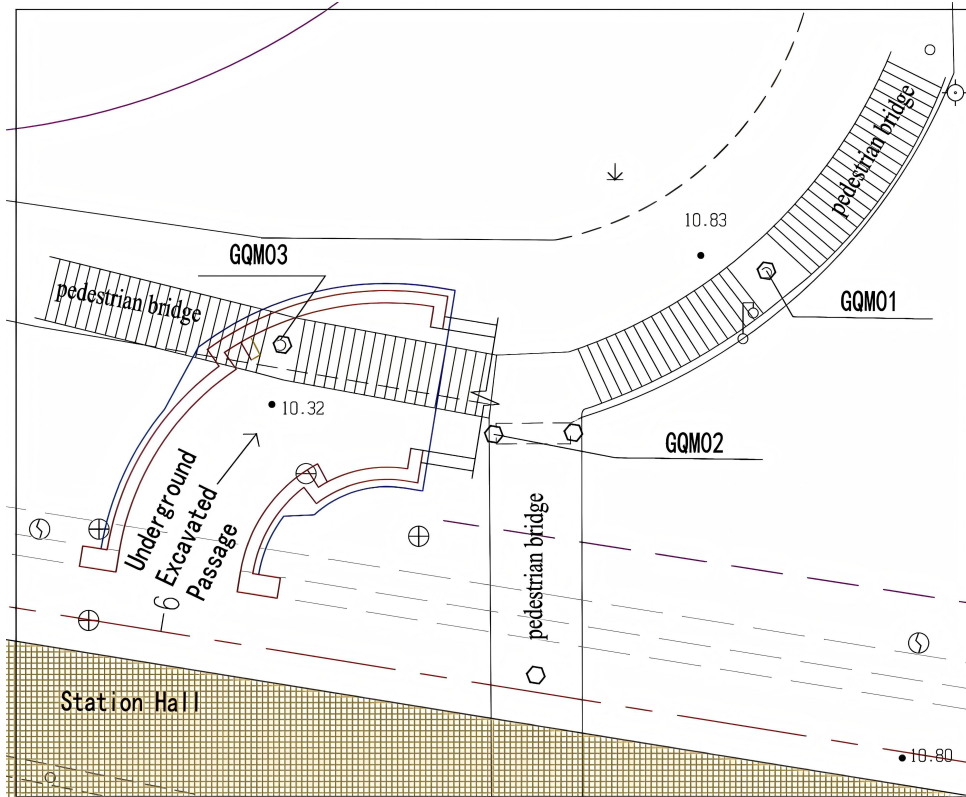
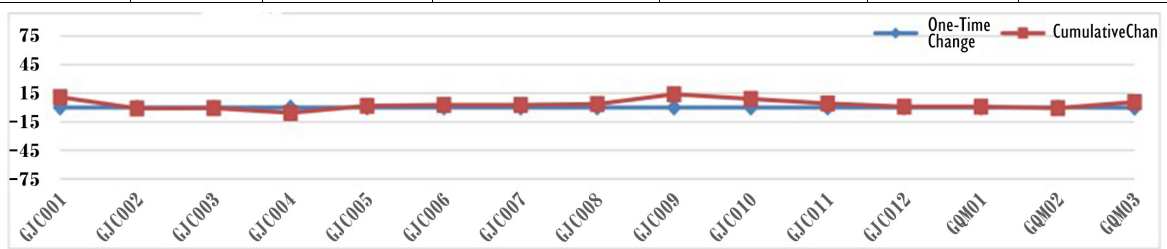


Figure 22. Monitoring and Finite Element Model Validation for the Pedestrian Bridge

Table 15. Monitoring and Finite Element Model Validation for Pedestrian Bridge

Monitoring Point No	Initial Value (m)	Current Change (mm)	Previous Cumulative Change (mm)	Current Cumulative Change (mm)	Change Rate (mm/d)	Remarks
GQM01	11.26387	0.03	0.95	0.98	0.03	Cumulative Monitoring Duration: 2117 Days
GQM02	13.56195	0.07	-0.76	-0.69	0.07	
GQM03	11.24065	-0.19	5.74	5.55	0.19	



Monitoring Data



The pedestrian bridge has been functioning normally since the construction was completed.

6. Conclusions

This study conducted in-depth exploration of the influence mechanism of subway station construction on the structural safety of adjacent pedestrian bridges and proposed targeted optimization strategies by establishing an integrated technical framework that combines three-dimensional finite element dynamic simulation, support structure optimization, and real-time on-site monitoring. The key conclusions are listed as follows:

(1) The integrated technical framework constructed in this study effectively overcomes the limitation of existing studies that only focus on a single aspect such as dynamic monitoring or finite element simulation. The composite support system composed of systematic anchor rods, lattice girders, and shotcrete performs excellently in controlling tunnel deformation. The maximum internal forces of the structure (bending moment: 157.7 kN m, shear force: 331.1 kN) are far below the bearing capacity limits specified in the Code for Design of Railway Tunnels (TB10003-2016), and the safety factor of the proposed support parameters is 22% higher than that of conventional schemes.

(2) The proposed coupled analysis method for subway construction and pedestrian bridge structural safety fully considers the dynamic construction process and realizes the quantitative assessment of construction impacts. With the improved support system, the difference in movement between neighboring piles is kept within 2.1 mm — far less than the code limit of 127 mm. Stress redistribution in the steel box girder is also limited to less than 15% of the allowed design value. These measures greatly reduce the impact of construction on the bridge structure.

(3) The optimized support system developed for complex strata (argillaceous siltstone and fully weathered silty clay) exhibits good adaptability. Geological sensitivity analysis shows that the fully weathered clay layer and moderately weathered argillaceous siltstone are the key strata affecting the support performance; this specific geological combination can reduce the displacement of the support structure by 18%–22%, which further verifies the rationality of the support system design in the target strata.

(4) Dynamic correction of the simulation model using real-time monitoring data significantly improves the accuracy of safety assessment. A comparative study on 12 construction stages shows that informatized construction technologies—such as the combination of real-time GNSS monitoring systems (with an accuracy of ± 1 mm) and 3D simulation—can dynamically adjust construction parameters, thereby reducing the deformation of the support structure by an additional 5%–8%. This provides a reliable guarantee for the safe construction of subway stations and the structural safety of adjacent pedestrian bridges.

(5) The methods and results proposed in this paper also show certain advantages compared to conventional

approaches. In this project, the differential settlement was controlled within 2.1 mm. This result is better than those usually seen in similar projects, thanks to the improved support system used here. Furthermore, the high consistency (92%) between the simulation results and field monitoring data underscores the improved accuracy of the modeling methodology adopted in this study, which benefits from the dynamic correction enabled by real-time data. The analysis also expands the scope of conventional assessments by considering the coupling effect of subway construction loads and crowd loads.

(6) It is emphasized that the research results can provide technical references for the design of support systems in similar subway construction projects, the formulation of pedestrian bridge protection measures, and the real-time safety monitoring of structures, and it is expected that the construction risk of adjacent structures can be reduced by 20%–30%.

Limitations: While achieving good results in the target project (Memorial Hall Station of Line 13) and specific strata (argillaceous siltstone and fully weathered silty clay), the study has limitations in stratum adaptability. For other complex strata (e.g., high-water-content sand layers, strongly weathered rock masses), subsequent studies need to adjust support parameters and simulation models based on stratum characteristics. Also, long-term environmental effects (e.g., soil creep) were not considered.

Future Research Directions: Future research should expand to other strata types, study the long-term performance of pedestrian bridges under the combined action of subway operation and environmental factors, develop a big data-based intelligent early warning system for structural safety, and adjust support parameters and simulation models for other complex strata to expand the application scope of research results.

Acknowledgements

First and foremost, I would like to convey my deepest gratitude to my supervisor, Dr. Boi-Yee Liao from the Department of Engineering, International College, Krirk University (Thailand), for her rigorous academic guidance, continuous encouragement, and patient support throughout my doctoral research and the preparation of this paper. Her professional insights and meticulous attitude have been fundamental to the completion of this work.

I am also sincerely thankful to China Railway Fourth Bureau Group Co., Ltd. for providing practical engineering resources, data support, and a collaborative research environment that laid the foundation for this study.

Additionally, I extend my appreciation to the faculty members and administrative staff of the Department of Engineering at Krirk University's International College for their assistance in facilitating academic exchanges and

research arrangements.

Finally, I am grateful to the anonymous reviewers for their constructive comments, which have greatly enhanced the quality of this manuscript.

REFERENCES

- [1] Zheng H, Yang G, Wei K, "Three-dimensional Finite Element Simulation Analysis of Urban Footbridge," *International Industrial Informatics and Computer Engineering Conference. XA, China, Jul., 2015*, pp. 1370-1373. DOI: 10.2991/IIICEC-15.2015.303.
- [2] Ji K, Liao B. "Investigation effect of metro entrance and exit construction on pedestrian overpass safety using numerical modelling and simulation," *Res. Eng. Struct. Mater.*, vol. 11, no. 5, pp. 2715-2730, 2025. DOI: 10.17515/resm2025-1084st0812rs.
- [3] Radim Nečas et al., "Tuned mass dampers -evaluation of the effect on two real footbridges," *ce/papers*, vol. 7, no. 3-4, pp. 100-105, 2024. DOI: 10.1002/CEPA.3073.
- [4] Jones Kimberly, Sun Min, Lin Cheng. "Numerical analysis of group effects of a large pile group under lateral loading," *Computers and Geotechnics*, vol. 144, p. 104660, 2022. DOI: 10.1016/j.compgeo.2022.104660.
- [5] Xue C, Psimoulis P A, "Monitoring the dynamic response of a pedestrian bridge by using low-cost GNSS receivers," *Engineering Structures*, vol. 284, p. 115993, 2023. DOI: 10.1016/j.engstruct.2023.115993.
- [6] ElSafty A, Okeil A, Fletcher J, et al., "Instrumentation and Strain Monitoring of BFRP Bars in Pedestrian Bridge Deck Link slab," *Journal of Physics: Conference Series*. vol. 2647, p. 182038, 2024. DOI: 10.1088/1742-6596/2647/18/182038.
- [7] Vasatko David et al., "Static Analysis of a Fully Composite Modular Footbridge," *Advances in Science and Technology*, vol. 147, no. 5, pp. 1-10, 2024. DOI: 10.4028/p-e4E3JO.
- [8] Kolacek Jan and Necas Radim and Velesik Marek, "Important Aspects Influencing the Dynamic Parameters of Slender Pedestrian Bridges Formed by Stress Ribbon Structure," *Advances in Science and Technology*, vol. 147, no. 5, pp. 21-32, 2024. DOI: 10.4028/p-4tZroN.
- [9] Hussein Muhammad et al., "Assessing structural health of ultra high-performance fiber reinforced concrete pedestrian bridges through OMA and FEM integration," *Structures*, vol. 69, p. 107331, 2024. DOI: 10.1016/j.istruc.2024.107331.
- [10] Castillo B, Marulanda J, Thomson P, "Innovative Experimental Assessment of Human-Structure Interaction Effects on Footbridges with Accurate Multi-Axial Dynamic Sensitivity Using Real-Time Hybrid Simulation," *Applied Sciences*, vol. 14, no. 19, p. 8908, 2024. DOI: 10.3390/app14198908.
- [11] Aux D J, Castillo B, Marulanda J, et al., "Modelling Human-Structure Interaction in Pedestrian Bridges Using a Three-Dimensional Biomechanical Approach," *Applied Sciences*, vol. 14, no. 16, p. 7257, 2024. DOI: 10.3390/app14167257.
- [12] Xin Chen et al., "Vibration serviceability assessment of ribbon-shaped large-span footbridge at high altitudes under wind-pedestrians coupling effects," *Structures*, vol. 66, p. 106885, 2024. DOI: 10.1016/j.istruc.2024.106885.
- [13] Li Z, Lan Y, Lin W, "Footbridge damage detection using smartphone-recorded responses of micromobility and convolutional neural networks," *Automation in Construction*, vol. 166, p. 105587, 2024. DOI: 10.1016/j.autcon.2024.105587.
- [14] Ministry of Communications of the People's Republic of China, *Code for Maintenance of Highway Bridges and Culverts: JTG H11-2004*, People's Transp. 2004, pp. 1-160.